Published online 30 June 2010 *Nucleic Acids Research, 2010, Vol. 38, No. 20* ***7167–7178***
doi:10.1093/nar/gkq588

Class-specific restrictions define primase interactions with DNA template and replicative helicase

Marilynn A. Larson[1,*], Mark A. Griep[2], Rafael Bressani[1], Kiran Chintakayala[3], Panos Soultanas[3] and Steven H. Hinrichs[1]

[1]Department of Pathology and Microbiology, University of Nebraska Medical Center, Omaha, NE 68198-5900, [2]Department of Chemistry, University of Nebraska-Lincoln, Lincoln, NE, 68588-0304, USA and [3]Centre for Biomolecular Sciences, School of Chemistry, University of Nottingham, Nottingham NG7 2RD, UK

Received March 30, 2010; Revised June 2, 2010; Accepted June 11, 2010

ABSTRACT

Bacterial primase is stimulated by replicative helicase to produce RNA primers that are essential for DNA replication. To identify mechanisms regulating primase activity, we characterized primase initiation specificity and interactions with the replicative helicase for gram-positive Firmicutes (*Staphylococcus, Bacillus* and *Geobacillus*) and gram-negative Proteobacteria (*Escherichia*, *Yersinia* and *Pseudomonas*). Contributions of the primase zinc-binding domain, RNA polymerase domain and helicase-binding domain on *de novo* primer synthesis were determined using mutated, truncated, chimeric and wild-type primases. Key residues in the β4 strand of the primase zinc-binding domain defined class-associated trinucleotide recognition and substitution of these amino acids transferred specificity across classes. A change in template recognition provided functional evidence for interaction in *trans* between the zinc-binding domain and RNA polymerase domain of two separate primases. Helicase binding to the primase C-terminal helicase-binding domain modulated RNA primer length in a species-specific manner and productive interactions paralleled genetic relatedness. Results demonstrated that primase template specificity is conserved within a bacterial class, whereas the primase–helicase interaction has co-evolved within each species.

INTRODUCTION

DNA replication is required by all autonomous organisms to duplicate and transmit their genetic material. During this process, the replicative helicase unwinds the chromosomal double helix while primase catalyzes the *de novo* synthesis of a template-directed RNA polymer at least once on the leading strand template and numerous times on the lagging strand template (1,2). Primase, encoded by *dnaG* in bacteria, provides RNA primers with a free 3′-hydroxyl group required by all known DNA polymerases. Extension of the RNA primers by the DNA polymerase holoenzyme results in the formation of Okazaki fragments of approximately 1000 to 2000 bases in bacteria (3).

The modular structure of bacterial DnaG primase includes an N-terminal zinc-binding domain (ZBD) that generally contains three cysteines and one histidine that coordinate the binding of a zinc ion (4,5). The central RNA polymerase domain (RPD) contains the active site where metal-dependent polymerization occurs (6). The C-terminal helicase-binding domain (HBD) of DnaG directly interacts with helicase (7–9). Fluorescence resonance energy transfer and *in vitro* activity assays indicated that two truncated primases can interact, suggesting that the extended ZBD from one primase binds to the DNA template within the RPD catalytic center of the other truncated protein (10).

Primases from both bacteriophages and bacteria initiate *de novo* primer synthesis on defined trinucleotides (11). The Firmicute primases from the Bacilli class, specifically *Staphylococcus aureus* and *Geobacillus stearothermophilus* (formerly known as *Bacillus stearothermophilus*), predominantly prime 5′-d(CTA) with moderate initiation on 5′-d(TTA) (12,13). DnaG from the γ-Proteobacteria *Escherichia coli* catalyzes primer synthesis on 5′-d(CTG) (14,15) and the Aquificae member *Aquifex aeolicus* initiates preferentially on 5′-d(CCC) (16).

Evidence to date suggests that the bacterial replicative helicase stimulates primase activity by acting as a platform for primase, thereby increasing the local concentration of

*To whom correspondence should be addressed. Tel: +1 402 559 9115; Fax: +1 402 559 5900; Email: malarson@unmc.edu

the ssDNA template (9,10,17). Stoichiometric analyses of this critical protein–protein interaction under saturating conditions indicate that three primases are present on each helicase hexamer (9,18). The helicase N-terminal domain directly interacts with the primase HBD (9,19–21), while the C-terminal domain of helicase is responsible for the hexameric quaternary structure and for hydrolyzing ATP (22,23). The functional interaction between the HBD and helicase N-terminal domain appears to be specific, since DnaG from *E. coli* and *S. aureus* are not stimulated by the heterologous helicase (12). Further, *E. coli* helicase is unable to productively interact with *B. anthracis* primase (24).

Important questions remain regarding the mechanistic process by which bacterial primases recognize specific trinucleotides, including whether this attribute is conserved within bacterial classes. Moreover, the evolutionary and functional relationship between the essential primase-helicase interaction has not been defined, nor is it known whether orthologs of these proteins from phylogenetic siblings can productively interact. To begin to address these questions and better understand the species-specific differences in primase and helicase, we functionally characterized these enzymes from multiple species within the divergent gram-positive Firmicutes and gram-negative Proteobacteria. Our findings suggest that core sequences in the primase ZBD predict template specificity within a bacterial class and that the primase HBD–helicase interaction has co-evolved despite differing environmental niches for mesophilic and thermophilic bacteria.

MATERIALS AND METHODS

Strains and nucleic acids

Bacterial strains were obtained from ATCC (*B. anthracis* Sterne and *Pseudomonas aeruginosa* PA01) or from the Armed Forces Institute of Pathology following the requirements of the Select Agent Program as outlined in the APHIS/CDC Form 2 (*Yersinia pestis* CO92) or as previously published (*S. aureus*, *E. coli* and *G. stearothermophilus*) (12,25,26). All manipulations of viable *Y. pestis* material were performed by authorized individuals within BSL-3 laboratories verified for select agent work using laboratory biosafety criteria as required. The *E. coli dnaG* mutant CR34/308 was obtained from the Coli Genetic Stock Center at Yale University. RNA standards were synthesized by Invitrogen and deoxyribonucleotide templates and PCR primers were generated by Integrated DNA Technologies.

Cloning and sequence analysis of primases and helicases

Primase and replicative helicase from *G. stearothermophilus* were cloned as previously described (25,26). Cloning strategies used for the construction of the truncated, chimeric and wild-type primases, as well as replicative helicases are described in the Supplementary Data and the PCR primers are listed in Supplementary Table S3. Nucleotide sequencing was performed by the UNMC Molecular Biology Core Facility. Sequences were aligned using the BESTFIT and PILEUP programs in the Wisconsin Package computation software (Accelrys Inc.) and/or ClustalW2.

Expression and purification of primases and helicases

Geobacillus stearothermophilus primase and replicative helicase expression and purification were performed as previously described (25,26). Truncated, chimeric, mutated and wild-type primases, as well as replicative helicases were expressed in *E. coli* BL21(DE3) and purified by nickel affinity chromatography as suggested by the manufacturers (Novagen EMD Biosciences, GE Healthcare). Enzyme purity and concentration were determined by 10% (w/v) SDS–PAGE analysis and spectrophotometry using the appropriate ϵ at 280 nm (Supplementary Table S4) and determined to be greater than 98% pure.

Site-directed mutagenesis of primase

Site-directed mutagenesis of the *S. aureus* primase ZBD was carried out using the QuikChange Multi Site-directed Mutagenesis Kit (Stratagene) with the appropriate oligonucleotides according to the manufacturer's recommendations. The presence of desired mutations and the absence of spurious mutations were confirmed by DNA sequencing.

RNA primer synthesis assay and thermally denaturing HPLC analysis

Reaction conditions and mixtures for mesophilic primases were used as previously optimized for *S. aureus* and *E. coli* with 400 μM of each NTP (12,27). Assay conditions for optimum *G. stearothermophilus* primase activity were determined using 1 mM of each NTP. All RNA primer synthesis reactions were performed in 100 μl nuclease-free water containing 50 mM HEPES, 100 mM potassium glutamate, 10 mM DTT, 10 mM magnesium acetate, and 2 μM of the designated template. Priming reactions contained 3.6 μM primase, unless otherwise noted, and were incubated for 1 h at the optimum temperature for primer synthesis. Reactions containing DnaG from mesophilic bacteria were incubated at 30°C and from thermophilic *G. stearothermophilus* at 50°C or 37°C in the absence or presence of helicase, respectively. Samples were processed as previously described using HPLC under thermally denaturing conditions at 80°C (16). Retention times of the primers were correlated to the retention times of the appropriate RNA standard (Supplementary Table S5) to confirm composition and length. RNA primers were quantified by using the ssDNA template as an internal control to normalize for system variability. All reactions were performed in triplicate, a minimum of three independent experiments with at least two different protein preparations.

Phylogenetic analyses

Protein sequences were aligned using the default settings of ClustalW2. Each multiple sequence alignment of the full-length proteins or their domains was analyzed using

the SEQBOOT program in PHYLIP 3.69 package to generate 100 random trees per data set. The PRODIST algorithm was then utilized to generate distances for each new random bootstrap tree and the FITCH program was used to minimize the distances. CONSENSE created a majority-rule consensus tree with bootstrap values. The final unrooted trees were created using the DRAWTREE program.

In vivo complementation assay

The *E. coli* CR34/308 RPD mutations P207L and Q252L in the *dnaG* allele were confirmed by PCR amplification and subsequent DNA sequencing of the cloned amplicon. To test complementation, *E. coli dnaG* mutant CR34/308 was transformed with the designated expression plasmid by electroporation. Equal amounts of the transformation mixture were plated for growth on LB agar plates supplemented with 0.36% glucose and 0.01% thiamine and assessed after overnight incubation at either the permissive temperature of 30°C or the nonpermissive temperature of 42°C. Untransformed and transformed cells were plated on both supplemented LB agar plates with or without kanamycin to confirm selection for those cells containing the kanamycin-resistant expression plasmid and incubated at both temperatures.

RESULTS

Trinucleotide initiation specificity for primase is class-specific

Based on earlier studies demonstrating that DnaG primase from gram-positive *S. aureus* and *G. stearothermophilus* initiated RNA primer synthesis from d(CTA) and d(TTA) and that the initiation trinucleotide for gram-negative *E. coli* was d(CTG), we hypothesized that trinucleotide initiation specificity would be restricted at the bacterial class level. To test this question, DnaG from the Bacilli Firmicute *B. anthracis* and the γ-Proteobacteria *Y. pestis* and *P. aeruginosa* were first evaluated in our template screening assay that tests initiation on all 64 possible trinucleotides. RNA polymer synthesis and the resulting lengths of these products were assessed to predict possible initiation trinucleotides. DNA templates with the sequence 5′-CAGA$(CA)_5$ XYZ $(CA)_3$, where XYZ is the trinucleotide of interest, were then used in the primer synthesis assay to confirm initiation specificity (Figure 1A). The RNA products were analyzed by thermally denaturing high-performance liquid chromatography (HPLC), a methodology that provides more precise qualitative and consistent quantitative data than traditional gel electrophoresis with radiolabeled NTPs (28).

As shown in Figure 1B, the gram-positive *B. anthracis* primase preferentially initiated from d(CTA) and to a slightly lesser degree on d(TTA), similar to the primases from *S. aureus* and *G. stearothermophilus*. For both the d(CTA) and d(TTA) templates, the major primer product synthesized by *B. anthracis* DnaG was a full-length 16-mer, with the former RNA polymer eluting earlier, consistent with its more hydrophilic composition. The primases from gram-negative *Y. pestis* and *P. aeruginosa* preferentially primed on d(CTG) and to a slightly reduced extent on d(CTA) (Figure 1C and D). Although *E. coli* DnaG was known to initiate on d(CTG), d(CTA) was also recognized (Figures 2A and 3A; Supplementary Figure S1), concurring with *in vivo* analyses in which the majority of RNA primers began with the sequence 5′-pppAG (29). Therefore, d(CTA) serves as a common initiation trinucleotide for DnaG from both the Firmicutes and Proteobacteria, representing a possible ancestral link with the presumably antecedent Firmicute clade. These data demonstrate that trinucleotide recognition by primase within these bacterial classes is conserved.

CTP titration experiments using the 23-mer CTA-specific template containing a single guanine at the antepenultimate position (Figure 1A) were performed to determine the initial nucleotide copied. The absence of CTP resulted in the predominant synthesis of a 13-mer RNA product, while increasing the CTP concentration decreased synthesis of the 13-mer with a concurrent increase in the full-length 16-mer primer (Supplementary Figure S2). A minor amount of RNA polymers longer than 13 ribonucleotides were also observed in the absence of CTP due to nucleotide misinsertion, a fidelity aspect shared by the primases from *S. aureus* and *E. coli* (27,30). These results indicate that DnaG from *B. anthracis*, *Y. pestis* and *P. aeruginosa* initiate from the middle nucleotide in the recognition trinucleotide, analogous to other fully characterized bacterial primases.

Primase ZBD and RPD interactions determine initiation of RNA primer synthesis

Experiments using the *E. coli*, *A. aeolicus* and T7 systems showed that the ZBD and RPD were sufficient to catalyze template-directed oligoribonucleotide synthesis (10,16,31). However, the potential influence of the HBD on primase specificity has not been examined. We found that the *S. aureus* and *E. coli* primases without their HBD produced RNA primers that were qualitatively and quantitatively similar to their wild-type equivalent, with the exception of truncated *E. coli* primase on d(CTG) (Supplementary Figure S1). HBD-swapped *S. aureus* and *E. coli* primases retained trinucleotide specificity of the respective ZBD+RPD; however, differences in primer synthesis efficiency were observed (Figure 2A–C). Collectively, these data demonstrate that neither the HBD of *S. aureus* nor *E. coli* primases regulates class-specific trinucleotide recognition.

The exchange of the ZBD between a Firmicute and Proteobacteria was predicted to transfer template specificity. To examine whether the ZBD was solely responsible for recognition of the initiation site, we tested the activity of a chimera that contained the ZBD of *S. aureus* DnaG and the RPD+HBD of *E. coli* primase. No priming occurred on templates containing the preferred Proteobacterial trinucleotide d(CTG); however, initiation did occur on d(CTA) and to a considerably lesser degree on d(TTA) (Figure 3A). A minor amount of primers that were longer than the expected 16-mer were synthesized on templates containing either d(CTA) or d(TTA), indicating

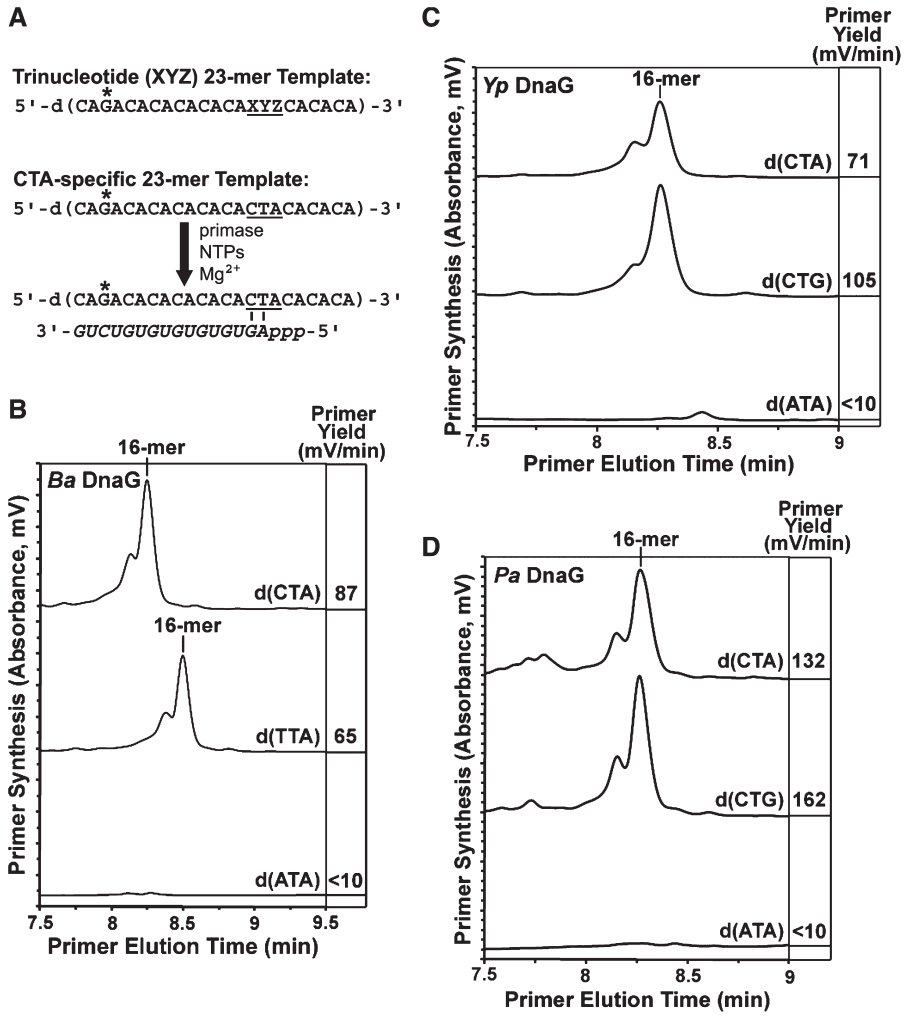

Figure 1. Trinucleotide initiation specificity for primases from *B. anthracis*, *Y. pestis* and *P. aeruginosa*. (**A**) Schematic of primase activity assay using the 23-mer trinucleotide-specific template where XYZ is the trinucleotide of interest (upper sequence) and with RNA primer synthesis initiating from the middle nucleotide of d(CTA) (lower sequence). The initiation trinucleotide in the ssDNA sequence is underlined, the full-length template-derived primer product is italicized and the unique guanine used to determine the initial nucleotide copied in the RNA primer is denoted with an asterisk. (**B–D**) Initiation specificity of DnaG primase on various trinucleotide-specific templates and detection of RNA primer products by denaturing HPLC. Chromatograms show the synthesis of RNA primers by *B. anthracis* (*Ba*) primase, *Y. pestis* (*Yp*) primase and *P. aeruginosa* (*Pa*) primase on 23-mer templates containing the recognition trinucleotides d(CTA), d(TTA) or d(CTG), as well as a representative negative template d(ATA). The elution of full-length 16-mer primers initiating from the middle nucleotide in the initiation trinucleotides d(CTA), d(CTG) or d(TTA) are shown and were based on the respective RNA standard. Each increment on the *y*-axis is equivalent to 5 mV absorbance at 260 nm.

that non-specific initiation occurred 3′ to these trinucleotides. This additional priming reflected the activity observed for wild-type *E. coli* DnaG and the enzymes containing the *E. coli* RPD, differing from the high specificity observed for wild-type *S. aureus* primase (Figures 2 and 3A; Supplementary Figure S1). Several studies have determined that relatively rigid polymerase active sites exhibit higher specificity than flexible catalytic centers (32–34). Therefore, the promiscuous priming observed for *E. coli* DnaG may be due to a slightly more flexible RPD active site relative to other bacterial primases.

Overall, the negligible initiation on d(TTA) and the lack of primer synthesis on d(CTG) demonstrated that neither the presence of the *S. aureus* ZBD nor the *E. coli* RPD+HBD are independently sufficient to confer class-associated trinucleotide initiation specificity. These findings indicate that a heterologous ZBD and RPD must interact in a precise manner for specific and significant initiation. In addition, template recognition must be determined by either critical amino acids in both the cognate ZBD and RPD or alternatively, key residues are located in only one of these domains.

Key residues in the ZBD β4 strand confer trinucleotide specificity

The ZBD crystal structure from *G. stearothermophilus* revealed a number of conserved basic and hydrophobic residues on the outer or exposed surface of the

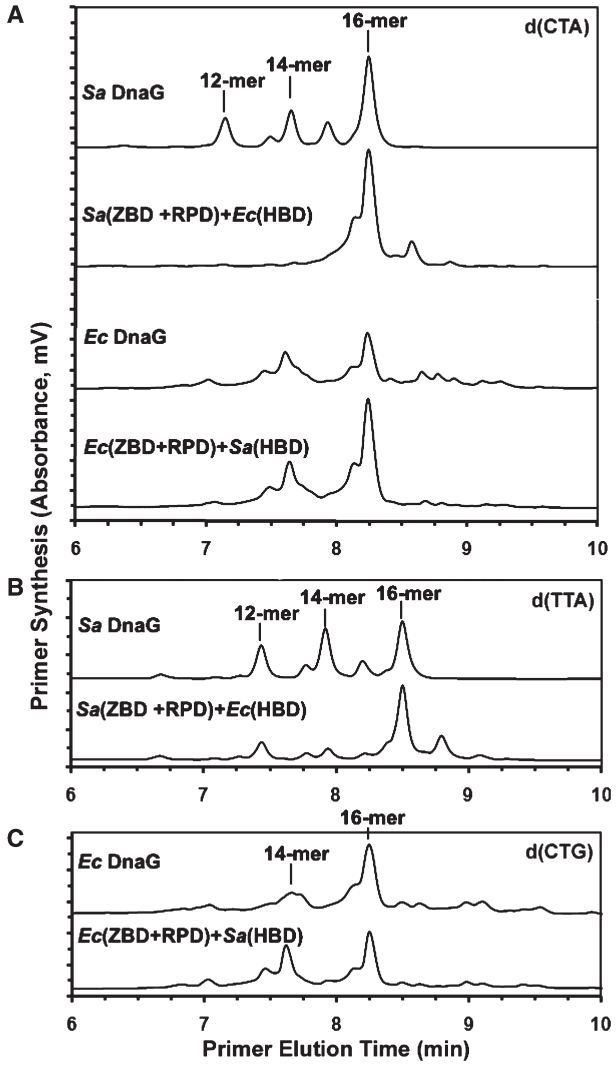

Figure 2. Contribution of the primase HBD on initiation specificity. (**A–C**) Comparison of primer synthesis by wild-type DnaG from *S. aureus* (*Sa*) and *E. coli* (*Ec*) to chimeric primases in which the HBD was exchanged. Primases were tested with the 23-mer template containing (A) d(CTA), (B) d(TTA) or (C) d(CTG) as designated in the upper right corner. RNA primers were visualized by denaturing HPLC and their nucleotide lengths were determined by comparison to 12-mer, 14-mer and 16-mer RNA size markers as indicated. Y-axis increments are each equal to 5 mV.

β sheet (4). We hypothesized that residues in the ZBD β sheet, conserved within members of the Firmicutes or Proteobacteria, and spatially located such that they potentially interact with the ssDNA template, contribute to class-associated trinucleotide specificity. To test this possibility, a sequence alignment of the ZBD from those primases with known initiation specificity was created using an algorithm that clustered the primases into their respective bacterial class. This alignment identified residues in the β sheet that were conserved between members of either the Firmicutes or Proteobacteria (Figure 3B). To assess the contribution of these residues and several other prospective amino acids on template specificity, *S. aureus* DnaG mutants were created by converting the ZBD residue to the corresponding amino acid in Proteobacterial primases (R32K, L37C, I56F, C57Y, E28K and D42H).

All *S. aureus* ZBD mutants were initially tested with the two screening templates that together comprise all 64 possible trinucleotides to evaluate enzyme activity and to determine if a new specificity was created. Template specificity was then confirmed using a 23-mer trinucleotide-specific template in the RNA priming assay (Figure 1A). All of the single-residue ZBD mutants exhibited the highest activity on the d(CTA) template, indicating that none of these amino acids alone were capable of changing the initiation specificity (Figure 3C). Double and triple substitutions in the ZBD of *S. aureus* DnaG were also evaluated (I56F/C57Y, E28K/D42H, R32K/I35H, R32K/G65H and E28K/D42H/C57Y). Of these ZBD mutants, only the *S. aureus* I56F/C57Y mutant gained function on d(CTG) (Figure 3C). These findings confirm that these two adjacent amino acids in the ZBD β4 strand are the dominant residues conferring specificity, and that trinucleotide recognition and initiation can be transferred across bacterial classes by providing the appropriate residues in the same β sheet location.

Class-associated trinucleotide specificity regulates a *trans* interaction between the ZBD and RPD of chimeric primases

Structural and activity analyses by Berger and associates demonstrated that the ZBD of one truncated primase can interact with the RPD active site of a second truncated primase (10). Class-associated trinucleotide specificity and the construction of two chimeras with different activities provided for a direct examination of this phenomenon for full-length bacterial primases. The chimeric enzyme containing the *S. aureus* ZBD and *E. coli* RPD+HBD was capable of primer synthesis on templates containing d(CTA), but had little or no activity on the preferred Proteobacterial trinucleotide d(CTG) (Figures 3A and 4A). The second chimera comprised the *E. coli* ZBD and the *S. aureus* RPD+HBD had no intrinsic activity on d(CTG) (Figure 4B) or any template (not shown). Mixing studies were performed with the expectation that if the *E. coli* ZBD conferred template recognition and initiation in *trans*, then *de novo* primer synthesis should occur on d(CTG). As shown in Figure 4C and D, the addition of the inactive *E. coli* ZBD chimeric primase to the reaction containing the chimera with the *S. aureus* ZBD and the *E. coli* RPD+HBD resulted in the production of primers on d(CTG). Doubling the molar concentration of the chimeric primases resulted in a 3-fold increase in primer synthesis. The most plausible explanation for the gain in function on d(CTG) or change in template specificity was that the *E. coli* ZBD on the inactive chimera was functionally interacting in *trans* with the *E. coli* RPD on the other full-length chimeric primase.

A second phenomenon occurred that had been previously observed with *E. coli* DnaG in that helicase stimulation resulted in shorter primers (35). In the mixed chimera activity assays, the major RNA product was a

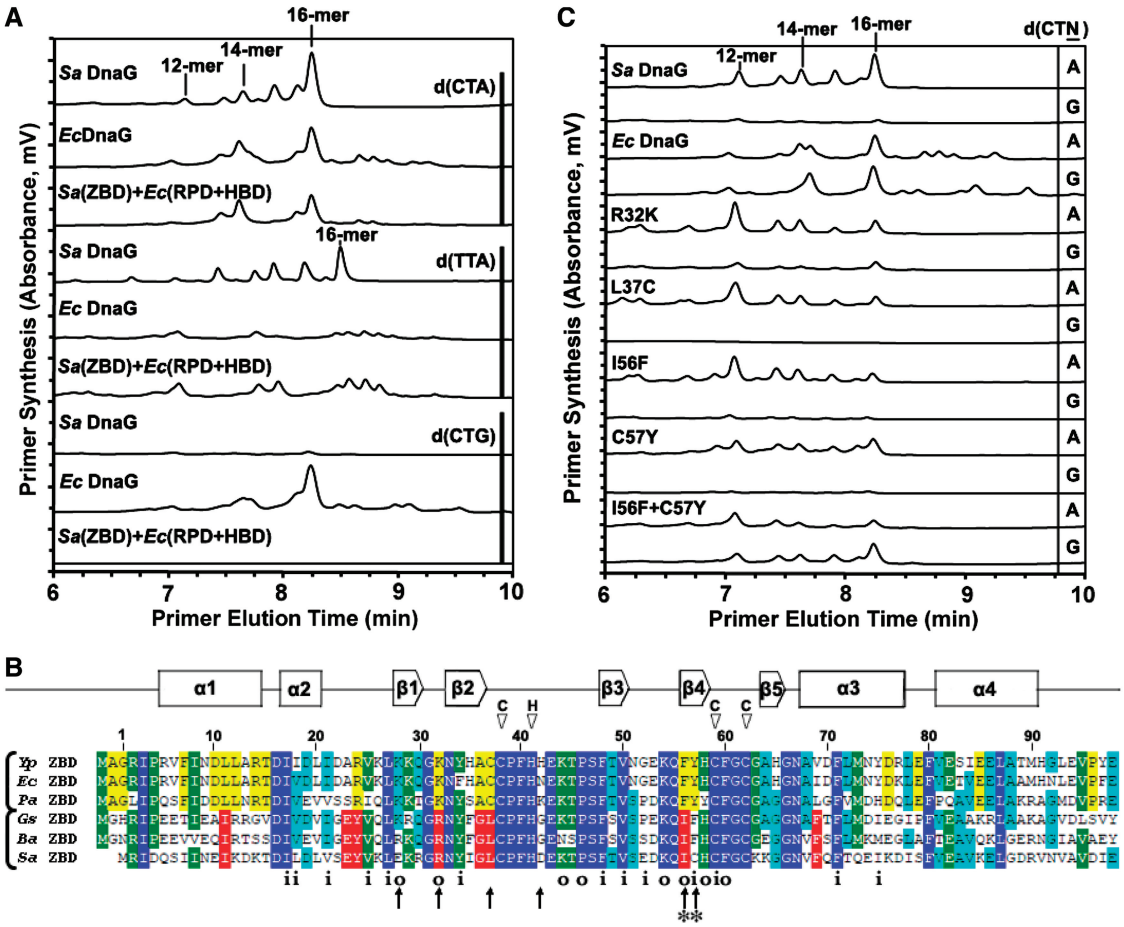

Figure 3. Key residues in the primase ZBD determine initiation specificity. (**A**) Denaturing HPLC analyses of RNA primers synthesized by the ZBD-swapped chimeric primase compared to wild-type primase from *S. aureus* (*Sa*) or *E. coli* (*Ec*) on templates containing d(CTA), d(TTA) or d(CTG). The 23-mer ssDNA template containing the specific trinucleotide is indicated on the right, with bold bars denoting common templates. Primer lengths are based on RNA size markers as shown. (**B**) Sequence alignment of the primase N-terminal ZBD from Gamma-proteobacteria and Bacilli Firmicutes with known trinucleotide initiation specificity. The ZBD residues are numbered above the alignment and are based on *S. aureus* DnaG (bottom sequence). Primases within the same bacterial class are bracketed on the left. Secondary structural elements are indicated above, and the unexposed inner (i) or exposed outer (o) amino acids are denoted below the relevant residues, as previously proposed (4). Open arrowhead indicates the location of the conserved cysteines and histidine. Solid arrow denotes the mutated *S. aureus* ZBD residues and asterisks indicate the mutated amino acids that confer trinucleotide specificity shown in (**C**). Identical residues conserved in all six (blue), five (green) or four (cyan) ZBDs are indicated. Conserved Gamma-proteobacteria (yellow) or Bacilli Firmicutes (red) ZBD residues are denoted. Abbreviations are *Yp*, *Y. pestis*; *Ec*, *E. coli*; *Pa*, *P. aeruginosa*; *Gs*, *G. stearothermophilus*; *Ba*, *B. anthracis*; and *Sa*, *S. aureus*. (C) Representative chromatograms showing RNA primer synthesis by the modified *S. aureus* primase with a single (R32K, L37C, I56F and C57Y) or a double (I56F/C57Y) ZBD mutation, as well as by wild-type DnaG from *S. aureus* (*Sa*) and *E. coli* (*Ec*). Priming assays were performed with the 23-mer template containing either d(CTA) or d(CTG) designated with an A or G, respectively, on the right. Primer lengths are indicated and each *y*-axis increment is equivalent to 10 mV.

14-mer rather than a full-length 16-mer (Figure 4C and D), similar to *E. coli* primer lengths *in vivo* (29). This result further substantiates the model that the intersubunit interaction restricts primer length and suggests an important mechanism that contributes to the regulation of primase processivity even in the absence of helicase.

Productive helicase stimulation of primase parallels genetic relatedness

Before testing the cross-reactivity of DnaG primases and replicative helicases within the same bacterial class, the primary sequence relatedness of each full-length protein and their associated domains were established for three Firmicutes and three Proteobacteria (Figure 5A–G; Supplementary Tables S1 and S2). The phylogenies of these full-length enzymes indicated there was a much stronger divergence between the Firmicute and Proteobacteria sequences for primase compared to replicative helicase (Figure 5A and B). The observed phyla split for DnaG is consistent with their template initiation specificities. Within each clade, the primases from *E. coli* and *Y. pestis* were the most similar followed by the primases from *G. stearothermophilus* and *B. anthracis* (Figure 5A; Supplementary Table S1). These findings suggested an evolutionarily conserved structural relationship that may translate into interchangeable functional activity. Based on these findings, we hypothesized that only primases and helicases that share considerable sequence homology within the interacting domains would cross-stimulate primer synthesis.

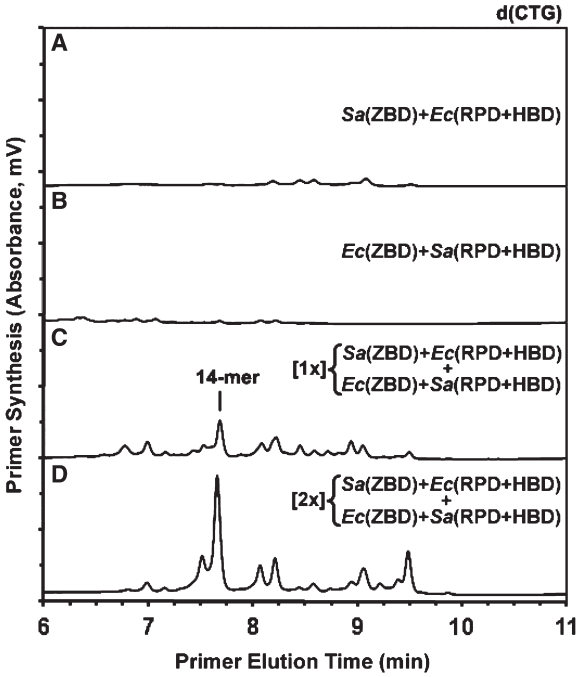

Figure 4. Full-length chimeric primases interact in *trans* on class-associated trinucleotides. (**A** and **B**) Representative chromatograms comparing RNA primer production on the Gamma-proteobacterial initiation trinucleotide d(CTG) by the chimeric primase comprising the *S. aureus* ZBD and *E. coli* RPD+HBD (A) or the chimera with the *E. coli* ZBD and *S. aureus* RPD+HBD (B). Priming reactions contained 3.6 μM chimeric primase. (**C** and **D**) Results of protein-mixing assays with the ZBD-swapped chimeras shown in (A) and (B) at a final concentration of (C) 1.8 μM or (D) 3.6 μM with the d(CTG)-containing 23-mer template. *Y*-axis increments are each equivalent to 5 mV.

To assess the evolutionary relationship of the domains that comprise DnaG and replicative helicase, the sequences for their associated domains were compared. Domain boundaries were based on published limited tryptic digestion studies and the resolved crystal structure for each domain. The phyla splits and branch lengths for the three primase domains were very similar to each other and to the full-length protein, despite their wide range of sequence similarities (Figure 5C–E; Supplementary Table S1). The ZBD had the greatest sequence identity and the HBD had the least. The strong phyla split for all three primase domains suggested that swapping domains between the two phyla would probably not result in a transfer of functionality. As was observed with full-length primase and the primase domain phylogenies (Figure 5A and C-E), the two helicase domain phylogenetic trees for the *E. coli* and *Y. pestis* clade branched the closest, followed by the *G. stearothermophilus* and *B. anthracis* clade (Figure 5F and G). Together these observations predicted that if heterologous stimulation was feasible, the highest level of functional cross-reactivity would occur between primase and helicase from these two pairs of bacteria.

Mixing experiments demonstrated that helicase from the Firmicutes *B. anthracis* and G. *stearothermophilus* cross-stimulated the heterologous primase for enhanced primer synthesis (Figure 5H). Similarly, DnaG and helicase from the Proteobacteria *E. coli* and *Y. pestis* productively interacted (Figure 5I). Interestingly, *Y. pestis* helicase stimulated *E. coli* primase to synthesize full-length primers rather than shorter RNA products, in contrast to the native *E. coli* DnaG–helicase interaction (Figure 5I). However, neither *S. aureus* nor *P. aeruginosa* was capable of productive interactions with other members of the same bacterial class (data not shown). Together these results indicate that genetic relatedness predicts the outcome of structure–function activity for helicase-stimulated primase activity.

Both *E. coli* and *S. aureus* helicase stimulation of DnaG results in a quantitative increase in the amount of primers produced, but RNA polymer lengths are reduced in *E. coli* (12,35). In this study, *B. anthracis*, *G. stearothermophilus*, *Y. pestis* and *P. aeruginosa* helicases stimulated their cognate primase to synthesize predominately full-length primers (Figure 5H and I; data not shown). Therefore, the *E. coli* helicase–DnaG interaction differs from other Proteobacteria and Firmicutes in terms of primer lengths produced. To investigate whether this effect was transferrable, both the *S. aureus* and *E. coli* HBD-swapped chimeric primases were tested with their cognate HBD-associated helicase. *S. aureus* helicase stimulated a modest increase in the production of predominantly full-length RNA primers by the chimeric primase containing the *E. coli* ZBD and RPD with the *S. aureus* HBD (Supplementary Figure S3A). In contrast, the chimera with the *S. aureus* ZBD and RPD and *E. coli* HBD synthesized shorter primers in the presence of *E. coli* helicase (Supplementary Figure S3B). These data demonstrate that the interplay between helicase and the cognate HBD modulates primer synthesis in a manner, mirroring the species-specific wild-type primase–helicase interaction.

In vivo complementation of an *E. coli* strain with a temperature-sensitive DnaG mutation

To determine whether RPD mutations could be rescued *in vivo*, we employed genetic complementation assays using the *E. coli* CR34/308 mutant carrying the thermosensitive *dnaG* allele. CR34/308 is a 'quick-stop mutant' that terminates DNA synthesis at the restrictive temperature of 42°C (36). This *E. coli dnaG* mutant contains two substitutions in the region that encodes the RPD, specifically P207L and Q252L. These conditional-lethal mutations in the catalytic core of this essential gene product allow for DNA replication to proceed at the permissive temperature of 30°C, but not at 42°C. Transformation of the empty plasmid did not rescue the mutant strain, whereas introduction of plasmid with *E. coli dnaG* permitted robust cell growth at the nonpermissive temperature of 42°C (Table 1). Moreover, transformation of the *E. coli dnaG* mutant with a plasmid expressing an N-terminally histidine-tagged *E. coli* DnaG rescued growth at 42°C, indicating that covalent linkage of the N-terminal tag does not affect the *in vivo* function of primase.

When genetic complementation assays were performed with plasmids expressing *Y. pestis*, *P. aeruginosa* or

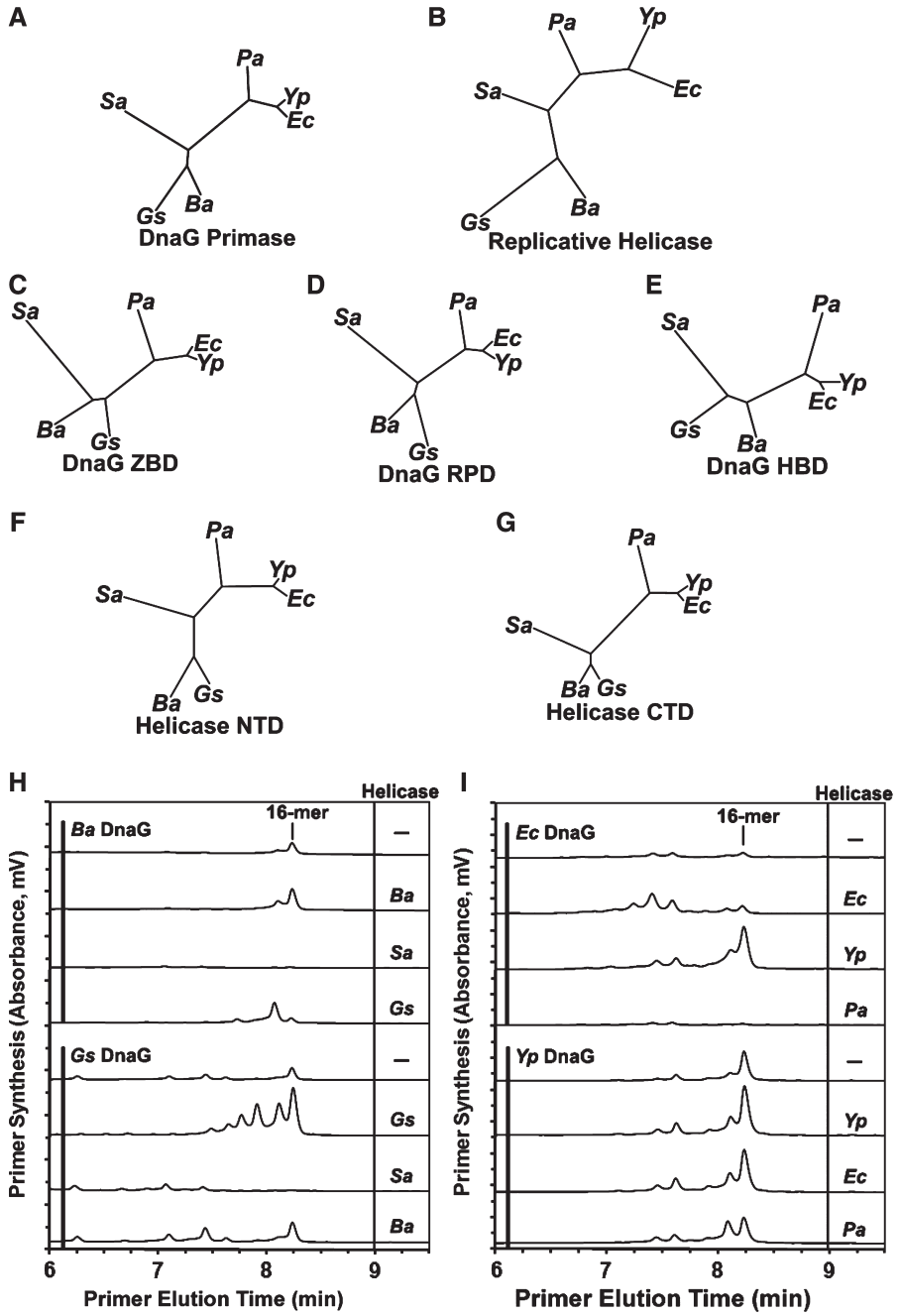

Figure 5. Cross-stimulation of primase activity by replicative helicases. (**A–G**) Unrooted phylogenetic trees based on sequence identities for DnaG primase and replicative helicase and their associated domains from the Bacilli Firmicutes *S. aureus* (*Sa*), *B. anthracis* (*Ba*) and *G. stearothermophilus* (*Gs*) and the Gamma-proteobacteria *E. coli* (*Ec*), *Y. pestis* (*Yp*) and *P. aeruginosa* (*Pa*). Phylogenetic trees for (A) full-length primase, (B) full-length helicase, (C–E) individual primase domains, the (F) helicase N-terminal domain (NTD) and (G) C-terminal domain (CTD) are shown. (**H**) RNA primer synthesis by DnaG primase from the Firmicutes *B. anthracis* and *G. stearothermophilus* in the absence or presence of a Firmicute replicative helicase at stoichiometric concentrations. Reactions were incubated with the 23-mer template containing d(CTA) and either 0.3 μM *B. anthracis* (*Ba*) DnaG (top four chromatograms) or 0.9 μM *G. stearothermophilus* (*Gs*) DnaG (bottom four chromatograms) without or with 0.1 μM or 0.3 μM of the designated Firmicute helicase hexamer, respectively. *Bacillus anthracis* and *G. stearothermophilus* DnaG activity assays contained either no helicase (–) or *B. anthracis* (*Ba*), *S. aureus* (*Sa*) or *G. stearothermophilus* (*Gs*) helicase as indicated on the right. (**I**) RNA primer synthesis by DnaG primase from the Proteobacteria *E. coli* and *Y. pestis* in the absence or presence of a Proteobacteria replicative helicase at stoichiometric concentrations. Reactions were incubated with the 23-mer template containing d(CTG) and either 1.8 μM *E. coli* (*Ec*) DnaG (top four chromatograms) or 0.6 μM *Y. pestis* (*Yp*) DnaG (bottom four chromatograms) without or with 0.6 μM or 0.2 μM of the designated Proteobacteria helicase hexamer, respectively. *E. coli* and *Y. pestis* DnaG activity assays contained either no helicase (–) or *E. coli* (*Ec*), *Y. pestis* (*Yp*), or *P. aeruginosa* (*Pa*) helicase as denoted on the right. Each *y*-axis increment is equivalent to 10 mV.

Table 1. *In vivo* complementation of an *E. coli* strain with a temperature-sensitive DnaG mutation[a]

Transformed expression plasmid	Growth at 30°C[b]	Growth at 42°C[c]
No plasmid	+	–
Empty plasmid	+	–
Escherichia coli DnaG primase[d]	+	+
Staphylococcus aureus DnaG primase	+	–
Yersinia pestis DnaG primase	+	+
Pseudomonas aeruginosa DnaG primase	+	–

[a]Representative overnight growth of untransformed or transformed *E. coli dnaG* mutant CR34/308 at the designated temperature.
[b]Permissive growth temperature.
[c]Non-permissive growth temperature.
[d]Untagged and N-terminally hexahistidine-tagged *E. coli* DnaG primase.

S. aureus primases, only expression of *Y. pestis* DnaG rescued the *E. coli dnaG* mutant strain at the restrictive temperature (Table 1). This *in vivo* result concurred with the *in vitro* experiments in which mutually productive cross-species stimulation of primer synthesis was obtained between primase and helicase from *E. coli* and *Y. pestis* (Figure 5I). These data indicate that primary sequence similarities directly correlate with the ability of primase and helicase from two different species to productively interact and function *in vivo*.

DISCUSSION

Class-restricted trinucleotide initiation specificity of bacterial primase

The demonstration of primase initiation on d(CTA) and d(TTA) for Firmicutes and d(CTG) and d(CTA) for Proteobacteria supports the general contention that members of the same phylogenetic class share trinucleotide template specificity. All three of these recognition trinucleotides code for leucine, an amino acid often determined to be among the most abundant in bacterial proteins. Given the high chromosomal skew for coding sequences, a high abundance of these three codons on the lagging strand template would provide a greater amount of initiation templates where primase acts. In each of these initiation sequence templates, the first two nucleotides are pyrimidines and the third is a purine. Initiation from these sequence motifs ensures that the first two primer NTPs are purines, bases known to stack strongly, thereby enhancing complex formation and subsequent dinucleotide condensation.

In the bacteriophage T7 primase, both Asp31 and His33 were determined to be essential for template specificity (37). Mutation of His33 to Ala altered synthesis at sequences containing a cryptic cytosine in the T7 primase recognition trinucleotide d(GTC) to d(GTA) and d(GTG). We determined that substitution of both Ile56 and Cys57 in the ZBD β4 strand of *S. aureus* DnaG to the Proteobacterial ZBD residues Phe and Tyr was required to switch specificity from d(CTA) to d(CTG). Similar to the findings in the T7 system, the preference for the cryptic third base in the initiation trinucleotide was altered. The spatial location of these two ZBD residues is on the surface of a β sheet proposed to bind ssDNA (Figure 6A) (4) and are structurally equivalent to Asp31 and His33 in the T7 primase. These key *S. aureus* and T7 ZBD residues are near the third residue (Cys) involved in zinc binding, indicating a conserved architecture for bacterial and bacteriophage primases and a possible communication between the zinc ion and nucleic acids.

Implications for *trans* interaction between the ZBD and RPD of primases

Productive crosstalk between primase subunits has been demonstrated in both the bacteriophage T4 and T7 by complementing catalytically inactive, full-length mutant primase with a truncated primase containing only the RPD (38,39). In bacterial systems, structural analyses suggested that primase without the HBD alternates between two different conformations: a compact form and an extended form (10). Our findings support the emerging paradigm for bacteria that the extended conformation of full-length DnaG is active and that the *trans* mode of interplay between subunits provides a regulatory mechanism by which site-specific primer initiation and elongation is restricted.

Even though each zinc finger domain in a classical zinc finger transcription factor recognizes and binds three nucleotides, three or more zinc finger domains are required for higher specificity and binding affinity to the 8 or 9 base pair recognition sequence. In the proposed model (Figure 6B), bacterial primase has a single zinc finger for sequence-specific recognition, binding and initiation that interacts in *trans* with the RPD on a separate primase. An exquisite level of specificity is achieved since the ZBD/RPD interaction can discriminate between a single nucleotide. Since hexameric helicase binds several primases, the close proximity of DnaG would further enhance ZBD and RPD intersubunit interactions.

Species specificity of primase-helicase interactions

Structural differences in the 5-bundle helix within the HBD of primase from the Firmicute *G. stearothermophilus* and the Proteobacteria *E. coli* have been determined (9,20,21). These differing structures, which must affect their orientation and flexibility, provide an explanation for the experimental absence of cross-stimulation between primases and helicases from these bacterial classes. Here we show that cross-stimulation between primase and helicase was restricted to closely related members of the same bacterial class, namely *E. coli* and *Y. pestis*, as well as *B. anthracis* and *G. stearothermophilus*. These results support a close ancestral relationship between these bacteria, despite their adaptation to diverse environments. This is particularly evident from the ability of the mesophilic *B. anthracis* helicase to stimulate thermophilic *G. stearothermophilus* primase and vice versa.

A comparison of the primase HBD and helicase interface from *G. stearothermophilus* with a *B. anthracis* model provided insight into residues that may be essential for the

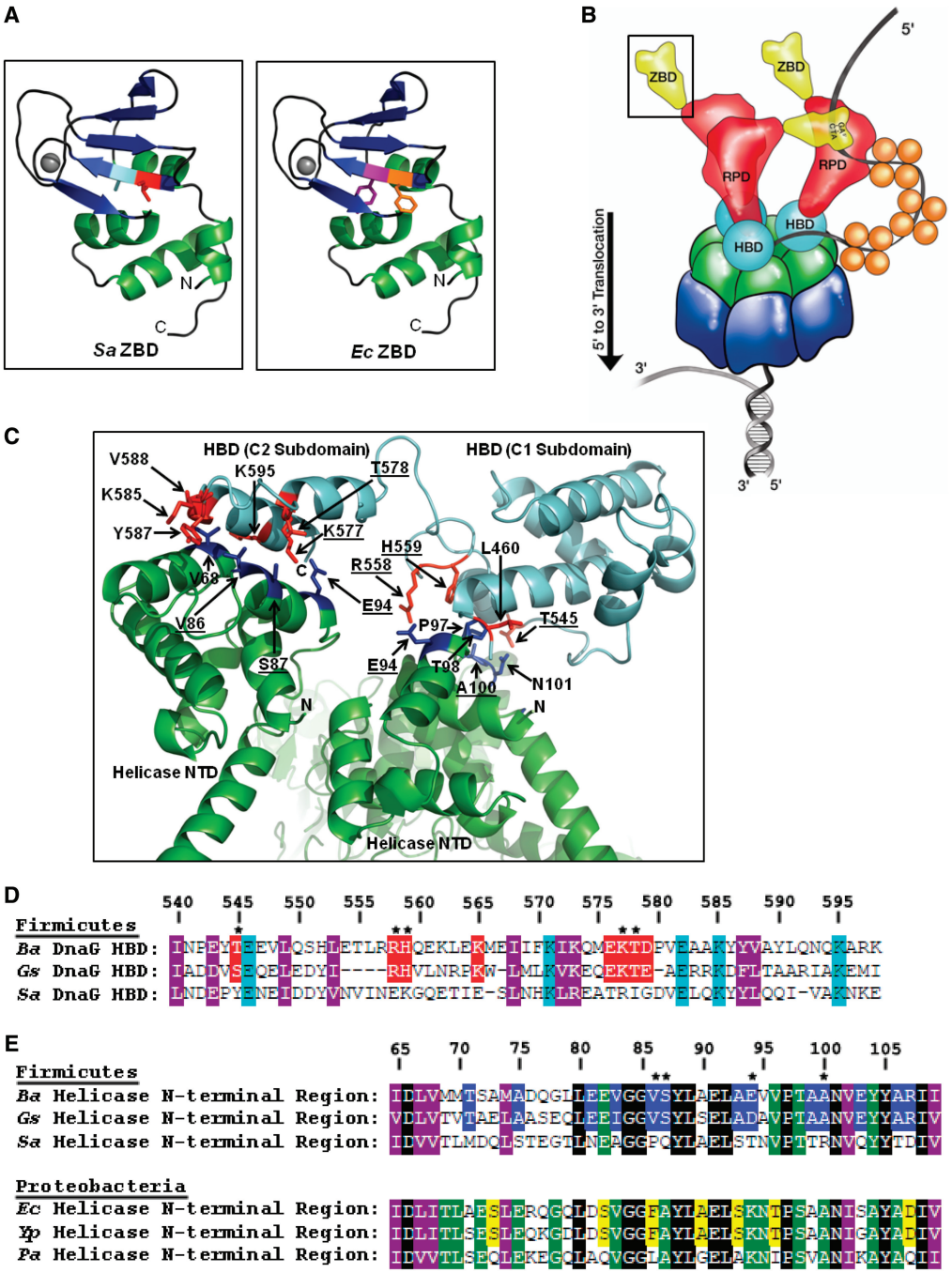

Figure 6. Regulation of primer synthesis by critical DnaG primase and replicative helicase residues. (**A**) Comparison of the *S. aureus* (*Sa*) and *E. coli* (*Ec*) primase ZBD models based on consensus structures obtained for *A. aeolicus* and *G. stearothermophilus* (PDB codes 2AU3 and 1D0Q, respectively). Two key residues in the β4 strand responsible for trinucleotide specificity are highlighted in red (Ile56) and cyan (Cys57) for the Firmicute *S. aureus* (left ZBD) and orange (Phe58) and purple (Tyr59) for the Proteobacteria *E. coli* (right ZBD). The zinc ion is shown as a gray sphere. All molecular structures were generated with the PyMOL molecular graphics software (http://pymol.sourceforge.net). (**B**) Model of *trans* interaction between primase ZBD (yellow) with adjacent RPD active site (red) on the class-associated trinucleotide d(CTA). Ribbon structure of boxed ZBD is shown in 6A. Arrow indicates direction of replication fork movement. The primase HBD (cyan) is shown interacting with replicative helicase N-terminal domain (green) that is covalently linked to the C-terminal ATPase domain (blue). SSB proteins (orange) are not shown to scale. (**C**) Interface between C1 and C2 subdomains of the primase HBD (cyan) and N-terminal domain (NTD) of two replicative helicase protomers (green) from *B. anthracis*. Models are based on *G. stearothermophilus* structures (PDB code 2R6C) and numbering refers to the *B. anthracis* proteins. Residues unique (underlined) and conserved in *B. anthracis* and *G. stearothermophilus* that potentially contribute to the productive cross-interaction between DnaG (red) and helicase (blue) are shown. (**D**) Multiple sequence alignment of the HBD region shown in (C) from the Bacilli Firmicutes *B. anthracis* (*Ba*), *G. stearothermophilus* (*Gs*) and *S. aureus* (*Sa*). Residues unique to *B. anthracis* and *G. stearothermophilus* are highlighted in red. Asterisk identifies residues underlined in (C). Identical (cyan) and similar (purple) amino acids conserved in all three Firmicutes are shown. (**E**) Multiple sequence alignments of the N-terminal region of helicase shown in (C) from the Bacilli Firmicutes *B. anthracis* (*Ba*), *G. stearothermophilus* (*Gs*) and *S. aureus* (*Sa*) and the Gamma-proteobacteria *E. coli* (*Ec*), *Y. pestis* (*Yp*) and *P. aeruginosa* (*Pa*). Identical amino acids unique to *B. anthracis* and *G. stearothermophilus* (blue), as well as *E. coli* and *Y. pestis* (yellow) are shown. Asterisk indicates residues underlined in (C). Amino acids conserved in either Firmicutes or Proteobacteria (green) and identical (black) or similar (purple) residues conserved in both phyla are shown.

productive cross-species interaction (Figure 6C–E). Although a number of residues are conserved in the HBD–helicase interface for members of the same or both bacterial classes, several amino acids are unique to *B. anthracis* and *G. stearothermophilus*, as well as *E. coli* and *Y. pestis*. Studies investigating the contribution of these species-specific and the conserved amino acids within this critical interface should illuminate their impact on this essential protein–protein interaction.

E. coli helicase stimulated *E. coli* DnaG to synthesize shorter rather than full-length primers, unlike the other productive bacterial helicase–primase interactions. A recent study suggested that differences in electrostatic potential surface charge on the N-terminal domain of *E. coli* helicase compared to another gram-negative bacteria may influence the binding stability to DnaG (40). This comparatively low negative charge distribution on the *E. coli* helicase N-terminal domain may contribute to the observed functional differences. However, *in vivo* complementation of the *E. coli dnaG* RPD mutant by *Y. pestis* DnaG and *in vitro* cross-stimulation between the primases and helicases from *E. coli* and *Y. pestis* demonstrates a degree of plasticity.

The productive interaction between DnaG and the replicative helicase hexamer has emerged as a critical element in the coordination of leading and lagging strand DNA synthesis (41). Our analyses of the interactions between primase and ssDNA and primase and helicase have revealed a series of properties that influence either class- or species-specific function. These key functional similarities and differences are controlled by the modular components of primase and have important evolutionary implications for the regulation of DNA replication. Since both primase and helicase are essential for cell propagation and survival, only those mutations that are either neutral or enhance functional activity will persist. The conserved mechanism by which primase recognizes specific sequence motifs and initiates *de novo* primer synthesis indicates that few mutations are tolerated in the primer-synthesizing domains. Additional studies on the molecular mechanisms that regulate primase activity and helicase–primase interactions will improve our understanding of the evolution of species-specific functions.

SUPPLEMENTARY DATA

Supplementary Data are available at NAR Online.

ACKNOWLEDGEMENTS

We thank Amanda Bartling and Matthew Shortridge for assistance with data collection, and Oluwatoyin Asojo for technical help with PyMOL software.

FUNDING

The Defense Advanced Research Program Agency (Award W911NF0510275 to S.H.H.); Biotechnology and Biological Sciences Research Council (Award E004717/1 to P.S.). Funding for open access charge: The Department of Pathology and Microbiology, University of Nebraska Medical Center.

Conflict of interest statement. None declared.

REFERENCES

1. Kornberg,A. and Baker,T. (1992) *DNA Replication*, 2nd edn. San Francisco, Freeman.
2. Okazaki,R., Okazaki,T., Sakabe,K., Sugimoto,K. and Sugino,A. (1968) Mechanism of DNA chain growth: I. Possible discontinuity and unusual secondary structure of newly synthesized chains. *Proc. Natl Acad. Sci. USA*, **59**, 598–605.
3. Wu,C.A., Zechner,E.L., Reems,J.A., McHenry,C.S. and Marians,K.J. (1992) Coordinated leading- and lagging-strand synthesis at the *Escherichia coli* DNA replication fork: V. Primase action regulates the cycle of Okazaki fragment synthesis. *J. Biol. Chem.*, **267**, 4074–4083.
4. Pan,H. and Wigley,D.B. (2000) Structure of the zinc-binding domain of *Bacillus stearothermophilus* DNA primase. *Structure*, **8**, 231–239.
5. Griep,M.A. and Lokey,E.R. (1996) The role of zinc and the reactivity of cysteines in *Escherichia coli* primase. *Biochemistry*, **35**, 8260–8267.
6. Godson,G.N., Schoenich,J., Sun,W. and Mustaev,A.A. (2000) Identification of the magnesium ion binding site in the catalytic center of *Escherichia coli* primase by iron cleavage. *Biochemistry*, **39**, 332–339.
7. Bird,L.E., Pan,H., Soultanas,P. and Wigley,D.B. (2000) Mapping protein–protein interactions within a stable complex of DNA primase and DnaB helicase from *Bacillus stearothermophilus*. *Biochemistry*, **39**, 171–182.
8. Chang,P. and Marians,K.J. (2000) Identification of a region of *Escherichia coli* DnaB required for functional interaction with DnaG at the replication fork. *J. Biol. Chem.*, **275**, 26187–26195.
9. Bailey,S., Eliason,W.K. and Steitz,T.A. (2007) Structure of hexameric DnaB helicase and its complex with a domain of DnaG primase. *Science*, **318**, 459–463.
10. Corn,J.E., Pease,P.J., Hura,G.L. and Berger,J.M. (2005) Crosstalk between primase subunits can act to regulate primer synthesis in *trans*. *Mol. Cell*, **20**, 391–401.
11. Frick,D.N. and Richardson,C.C. (2001) DNA primases. *Ann. Rev. Biochem.*, **70**, 39–80.
12. Koepsell,S.A., Larson,M.A., Griep,M.A. and Hinrichs,S.H. (2006) *Staphylococcus aureus* helicase but not *Escherichia coli* helicase stimulates S. aureus primase activity and maintains initiation specificity. *J. Bacteriol.*, **188**, 4673–4680.
13. Thirlway,J. and Soultanas,P. (2006) In the *Bacillus stearothermophilus* DnaB–DnaG complex, the activities of the two proteins are modulated by distinct but overlapping networks of residues. *J. Bacteriol.*, **188**, 1534–1539.
14. Yoda,K. and Okazaki,T. (1991) Specificity of recognition sequence for *Escherichia coli* primase. *Mol. Gen. Genet.*, **227**, 1–8.
15. Swart,J.R. and Griep,M.A. (1993) Primase from *Escherichia coli* primes single-stranded templates in the absence of single-stranded DNA-binding protein or other auxiliary proteins. Template sequence requirements based on the bacteriophage G4 complementary strand origin and Okazaki fragment initiation sites. *J. Biol. Chem.*, **268**, 12970–12976.
16. Larson,M.A., Bressani,R., Sayood,K., Corn,J.E., Berger,J.M., Griep,M.A. and Hinrichs,S.H. (2008) Hyperthermophilic *Aquifex aeolicus* initiates primer synthesis on a limited set of trinucleotides comprised of cytosines and guanines. *Nucleic Acids Res.*, **36**, 5260–5269.
17. Soultanas,P. (2005) The bacterial helicase–primase interaction: a common structural/functional module. *Structure*, **13**, 839–844.
18. Mitkova,A.V., Khopde,S.M. and Biswas,S.B. (2003) Mechanism and stoichiometry of interaction of DnaG primase with DnaB helicase of *Escherichia coli* in RNA primer synthesis. *J. Biol. Chem.*, **278**, 52253–52261.
19. Tougu,K., Peng,H. and Marians,K.J. (1994) Identification of a domain of *Escherichia coli* primase required for functional

interaction with the DnaB helicase at the replication fork. *J. Biol. Chem.*, **269**, 4675–4682.
20. Syson,K., Thirlway,J., Hounslow,A.M., Soultanas,P. and Waltho,J.P. (2005) Solution structure of the helicase-interaction domain of the primase DnaG: a model for helicase activation. *Structure*, **13**, 609–616.
21. Oakley,A.J., Loscha,K.V., Schaeffer,P.M., Liepinsh,E., Pintacuda,G., Wilce,M.C., Otting,G. and Dixon,N.E. (2005) Crystal and solution structures of the helicase-binding domain of *Escherichia coli* primase. *J. Biol. Chem.*, **280**, 11495–11504.
22. Biswas,E.E. and Biswas,S.B. (1999) Mechanism of DnaB helicase of *Escherichia coli*: structural domains involved in ATP hydrolysis, DNA binding, and oligomerization. *Biochemistry*, **38**, 10919–10928.
23. Nakayama,N., Arai,N., Kaziro,Y. and Arai,K. (1984) Structural and functional studies of the *dnaB* protein using limited proteolysis. Characterization of domains for DNA-dependent ATP hydrolysis and for protein association in the primosome. *J. Biol. Chem.*, **259**, 88–96.
24. Biswas,S.B., Wydra,E. and Biswas,E.E. (2009) Mechanisms of DNA binding and Regulation of *Bacillus anthracis* DNA primase. *Biochemistry*, **48**, 7373–7382.
25. Bird,L.E. and Wigley,D.B. (1999) The *Bacillus stearothermophilus* replicative helicase: cloning, overexpression and activity. *Biochim. Biophys. Acta*, **1444**, 424–428.
26. Pan,H., Bird,L.E. and Wigley,D.B. (1999) Cloning, expression, and purification of *Bacillus stearothermophilus* DNA primase and crystallization of the zinc-binding domain. *Biochim. Biophys. Acta*, **1444**, 429–433.
27. Swart,J.R. and Griep,M.A. (1995) Primer synthesis kinetics by *Escherichia coli* primase on single-stranded DNA templates. *Biochemistry*, **34**, 16097–16106.
28. Koepsell,S., Bastola,D., Hinrichs,S.H. and Griep,M.A. (2004) Thermally denaturing high-performance liquid chromatography analysis of primase activity. *Anal. Biochem.*, **332**, 330–336.
29. Kitani,T., Yoda,K., Ogawa,T. and Okazaki,T. (1985) Evidence that discontinuous DNA replication in *Escherichia coli* is primed by approximately 10 to 12 residues of RNA starting with a purine. *J. Mol. Biol.*, **184**, 45–52.
30. Koepsell,S.A., Larson,M.A., Frey,C.A., Hinrichs,S.H. and Griep,M.A. (2008) *Staphylococcus aureus* primase has higher initiation specificity, interacts with single-stranded DNA stronger, but is less stimulated by its helicase than *Escherichia coli* primase. *Mol. Microbiol.*, **68**, 1570–1582.
31. Frick,D.N., Baradaran,K. and Richardson,C.C. (1998) An N-terminal fragment of the gene 4 helicase/primase of bacteriophage T7 retains primase activity in the absence of helicase activity. *Proc. Natl Acad. Sci. USA*, **95**, 7957–7962.
32. Skopalik,J., Anzenbacher,P. and Otyepka,M. (2008) Flexibility of human cytochromes P450: molecular dynamics reveals differences between CYPs 3A4, 2C9, and 2A6, which correlate with their substrate preferences. *J. Phys. Chem. B*, **112**, 8165–8173.
33. Thorpe,I.F. and Brooks,C.L. 3rd (2007) Molecular evolution of affinity and flexibility in the immune system. *Proc. Natl Acad. Sci. USA*, **104**, 8821–8826.
34. Tokuriki,N. and Tawfik,D.S. (2009) Protein dynamism and evolvability. *Science*, **324**, 203–207.
35. Johnson,S.K., Bhattacharyya,S. and Griep,M.A. (2000) DnaB helicase stimulates primer synthesis activity on short oligonucleotide templates. *Biochemistry*, **39**, 736–744.
36. Grompe,M., Versalovic,J., Koeuth,T. and Lupski,J.R. (1991) Mutations in the *Escherichia coli dnaG* gene suggest coupling between DNA replication and chromosome partitioning. *J. Bacteriol.*, **173**, 1268–1278.
37. Kusakabe,T., Hine,A.V., Hyberts,S.G. and Richardson,C.C. (1999) The Cys4 zinc finger of bacteriophage T7 primase in sequence-specific single-stranded DNA recognition. *Proc. Natl Acad. Sci. USA*, **96**, 4295–4300.
38. Yang,J., Xi,J., Zhuang,Z. and Benkovic,S.J. (2005) The oligomeric T4 primase is the functional form during replication. *J. Biol. Chem.*, **280**, 25416–25423.
39. Lee,S.J. and Richardson,C.C. (2002) Interaction of adjacent primase domains within the hexameric gene 4 helicase-primase of bacteriophage T7. *Proc. Natl Acad. Sci. USA*, **99**, 12703–12708.
40. Kashav,T., Nitharwal,R., Abdulrehman,S.A., Gabdoulkhakov,A., Saenger,W., Dhar,S.K. and Gourinath,S. (2009) Three-dimensional structure of *N*-terminal domain of DnaB helicase and helicase-primase interactions in *Helicobacter pylori*. *PloS ONE*, **4**, e7515.
41. Tanner,N.A., Hamdan,S.M., Jergic,S., Loscha,K.V., Schaeffer,P.M., Dixon,N.E. and van Oijen,A.M. (2008) Single-molecule studies of fork dynamics in *Escherichia coli* DNA replication. *Nat. Struct. Mol. Biol.*, **15**, 170–176.